

THREE-DIMENSIONAL OF COASTAL FRONT RECONSTRUCTION USING RADARSAT-1 SAR SATELLITE DATA

Maged MARGHANY and Mazlan HASHIM

Institute of Geospatial Science and Technology (INSTeG)
Universiti Teknologi Malaysia
81310 UTM, Skudai, Johor Bahru, Malaysia,

E-mail: maged@utm.my,
: magedupm@hotmail.com

KEY WORDS: Fuzzy B-spline algorithm; 3D reconstruction; Front; RADARSAT-1 SAR; velocity bunching; Volterra model; and 3-D

Abstract: Natural phenomena that are imaged using remote sensing satellite data can be reconstructed in 3-D. This process can be accomplished either by active or passive methods. The active methods interfere with the reconstructed phenomena, either mechanically or radiometrically. The radiometric methods reconstruct the 3-D from the reflected or backscattered information about the specific objects or phenomena. However, passive methods use a sensor to measure the radiance reflected or emitted by the object's surface to infer its 3-D structure. 3-D reconstruction of natural phenomena plays tremendous role to understand a complex system such as the dynamic processes of coastal waters.

Three-dimensional (3D) computer visualization has tremendous demands for complex phenomena studies. Coastal waters are considered as complex system because of they are dominated by complex system. In this regard, this study aims to present a method that is based on fuzzy B-spline to reconstruct 3D of coastal water phenomena such as front from two-dimensional RADARSAT-1 SAR data. In doing so, fuzzy B-spline algorithm is integrated with Volterra model and velocity bunching model. Volterra algorithm is used to determine the sea surface current along the front zone while velocity bunching model implemented to acquire the information about significant wave height. fuzzy B-spline reconstructed 3-D front with smooth graphic feature. Indeed, fuzzy B-spline tracked the smooth and rough surface. Finally, fuzzy B-spline algorithm can keep track of uncertainty with representing spatially clustered gradient of flow points across the front. In conclusion, the fuzzy B-spline algorithm can be used for 3-D front reconstruction with integration of velocity bunching and Volterra algorithm.

INTRODUCTION

Front plays tremendous role to understand the mechanisms of coastal water circulation, marine productivities and coastal pollutant materials spreading (Simpson and Pingree 1978; Bowden 1983; Robinson 1995, Marghany 2011). Although, conventional methods for front studies depend on in-situ measurements of sea water temperature and salinity they might be costly and time consuming. Isothermal, isohaline contours and water mass diagrams are established procedures for front detection nevertheless front cannot be visualized in large scale surface ocean (Simpson 1981; Bowden 1983; Marghany 2012).

In this paper, we address how 3-D front can be reconstructed from single SAR data (namely the RADARSAT-1 SAR) using integration of Volterra kernel (England and Garello, 1990), velocity bunching and Fuzzy B-spline models (Marghany et al., 2010 and Marghany and Mazlan 2010). In this regard, synthetic aperture radar (SAR) is able to identify front as a result of abruptly changes of surface wave pattern across front led to exceedingly change cross backscatter of SAR data. Therefore, Johannessen et al., (1996) stated that SAR images can sometimes be used to interpret frontal dynamics, including growth and decay of meanders. Recently, Jiang et al., (2009) exploited various remote sensing data. Satellite images obtained from the Advanced Very High Resolution Radiometer (AVHRR), the Moderate Resolution Imaging Spectroradiometer (MODIS), the Sea-viewing Wide Field-of-view Sensor (SeaWiFS) and RADARSAT-1 SAR S1 mode data to study coastal water plume and front which is also captured in S1 mode data (Klemas 2011).

There are about three hypothesis that examined are: (i) the use of Volterra model to detect front flow pattern in RADARSAT-1 SAR C_{HH} band; (ii) the use of velocity bunching model to acquire significant wave height from RADARSAT-1 SAR data; and (iii) to utilize fuzzy B-spline to remodel 3-D of front surface. In fact, scientists have

used conventional mathematical algorithms to comprehend the complexity of various system interaction. In this regard, imaging coastal feature in synthetic aperture radar (SAR) required such standard mathematical algorithms have been reported recently by (Zaki, 2007; Messaoudi et al., 2007; Stephen 2009; Adeyemo and Fred 2009; Mehmet 2009; Ugwu, 2009; Akintorinwa and Adesoji 2009; Boumaza et al., 2009; Anjamrooz 2011; Anjamrooz et al., 2011; Khadijeh et al., 2011; Guillermo et al., 2011; Murat 2011; Mustafa 2011).

METHODS AND EQUATION

3D Model for front reconstruction

There are three algorithms involved for 3-D front reconstruction; Volterra, velocity bunching and Fuzzy B-spline algorithms. Significant wave heights are simulated from RADARSAT-1 SAR image by using velocity bunching model. Fuzzy B-spline used significant wave height information to reconstruct 3-D front. Moreover, front flow pattern is modeled by Volterra model. The RADARSAT-1 SAR fine mode data were acquired on March 26, 2004, over the coastline of Kuala Terengganu, Malaysia ($103^{\circ} 5' E$ to $103^{\circ} 9'E$ and $5^{\circ} 20' N$ to $5^{\circ} 27' N$). The RADARSAT-1 SAR fine mode data are acquiring information using C band HH polarized of frequency 5.3 GHz. The swath width of RADARSAT-1 SAR fine mode sensor is 50 km, with the range resolution of 8-9 km. There are two numbers of looks for The RADARSAT-1 SAR and the incident angle of 35° - 49° (RADARSAT 2012).

Volterra Model

In refereeing to Inglad and Garello, (1990), Volterra series can be used to model nonlinear imaging mechanisms of surface current gradients by RADARSAT-1 SAR image. As result of that Volterra linear kernel is contained most of RADARSAT-1 SAR energy which used to simulate current flow along range direction. Following Inglad and Garello, (1990) Volterra kernel filter has the following expression:

$$H_{1y}(v_x, v_y) = k_y \vec{U} \cdot \frac{\partial x}{\partial u_x} \left[\vec{K}^{-1} \left[\frac{\partial}{\partial t} + \frac{\partial \vec{c}_g}{\partial x} + \frac{\partial \vec{u}_x}{\partial x} + 0.043 \frac{(\vec{u}_a \vec{K})^2}{\omega_0} \right] \right] \left[\frac{\partial \psi}{\partial \omega} \right] \quad (1)$$

$$\frac{\vec{c}_g(\vec{K})\vec{U} + j.0.043(\vec{u}_a \vec{K})^2 \omega_0^{-1}}{[\vec{c}_g(\vec{K})\vec{U}]^2 + [0.043(\vec{u}_a \vec{K})^2 \omega_0^{-1}]^2} + j.(0.6.10^{-2} \cdot \vec{K}^{-4}) \left(\frac{R}{V} \right) \vec{u}_x$$

where \vec{U} is the mean current velocity, \vec{u}_x is the current flow while \vec{u}_a is current gradient along azimuth direction, respectively. k_y is the wave number along range direction, \vec{K} is the spectra wave number, ω_0 is the angular wave frequency, \vec{c}_g is the wave velocity group, ψ is the wave spectra energy and R/V is the range to platform velocity ratio. In reference to Inglad and Garello, (1990), the inverse filter $G(v_x, v_y)$ is used since $H_{1y}(v_x, v_y)$ has a zero for (v_x, v_y) which indicates the mean current velocity should have a constant offset. The inverse filter $G(v_x, v_y)$ can be given as

$$G(v_x, v_y) = \begin{cases} [H_{1y}(v_x, v_y)]^{-1} & \text{If } (v_x, v_y) \neq 0, \\ 0 & \text{otherwise.} \end{cases} \quad (2)$$

Using equation 2 into 3, range current velocity $U_y(0, y)$ can be estimated by

$$U_y(0, y) = I_{RADARSAT-1SAR} \cdot G(v_x, v_y) \quad (3)$$

where $I_{RADARSAT-1SAR}$ is the frequency domain of Radarsat-1 SAR image acquired by applying 2-D Fourier transform on RADARSAT-1 SAR image.

Velocity Bunching

Following Vachon (1994), the relation between standard deviation of the azimuth shift σ and significant wave height H_s can be given by

$$\sigma = \left(\frac{R}{V} \right) \left(1 - \frac{\sin^2(\theta)}{2} \right)^{0.5} \left(\frac{k_x g}{8} \right)^{0.5} H_s \quad (4)$$

where k_x is the azimuth wave number, θ is RADARSAT-1 SAR image incident angle, R/V is the scene range to platform velocity ratio and g is the acceleration due to the gravity. Note that the mean wave period T_0 is equal to $2\pi(\langle k_x \rangle g)^{-0.5}$. The significant wave height H_s can be obtained:

$$H_s = 0.6(\rho_{\zeta\zeta})^{0.5} \left[\frac{1 + \theta^2/4}{R/V} \right] T_0 \quad (5)$$

where θ is the RADARSAT-1 SAR incidence angle and equation 5 is used to estimate the significant wave height which is based on the standard deviation of the azimuth shift σ .

The Fuzzy B-splines Method

Fuzzy B-spline concept has adopted from Anile et al., (1995) and Anile (1997) which shows excellent 3-D reconstruction stated by Marghany et al., (2010) and Marghany and Mazlan (2011). Considering significant wave height modeled by using velocity bunching and radar backscatter cross section across front, fuzzy numbers are created. In doing so, two basic notions of confidence interval and presumption level are considered (Hassasi and Saneifard 2011 and Majid and Gondal 2011). A confidence interval is a real values interval which provides the sharpest enclosing range for significant wave height values. An assumption level μ -level is an estimated truth value in the [0,1] interval of significant wave height changes (Anile 1997). The 0 value suits to minimum knowledge of significant wave heights, and 1 to the maximum of significant wave height. A fuzzy number is then prearranged in the confidence interval set, each one related to an assumption level μ [0,1]. Additionally, the following must hold for each pair of confidence interval which define a number: $\mu > \mu' \Rightarrow h > h'$. Let us consider a function $f: h \rightarrow h$, of N fuzzy variables h_1, h_2, \dots, h_n . Where h_n is the global minimum and maximum values of significant wave heights. The construction begins with the same preprocessing to compress the measured significant wave height values into an uniformly spaced grid of cells. Then, a membership function is defined for each pixel which incorporates the degrees of certainty of radar cross backscatter.

RESULTS AND DISCUSSIONS

Figure 1 shows the F1 mode data which acquired along the coastal water of Kuala Terengganu, Malaysia on March 26, 2004. Figure 1 shows the signature of current boundary which can turn up as a result of brightness frontal curved line. Furthermore, it is clear that the front occurred close to estuary, which is a clear indications of tidal front events. In fact, the interaction of flood tidal current flow from estuary with topography can form a tidal front (Bowden 1983).

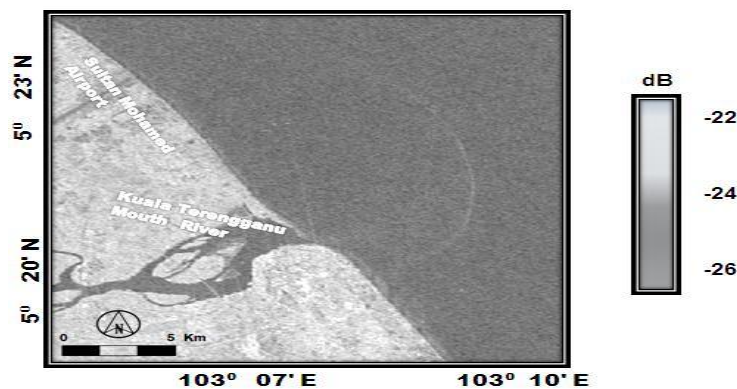


Figure 3: Backscatter variations in F1 mode data

The RADARSAT-1 backscatter cross-section across front has a maximum value of -21.25dB. According to Vogelzang et al.,(1997), ocean current boundaries are often accompanied by the changes in the surface roughness that can be detected by SAR. These interactions can cause an increase in the surface roughness and radar backscatter (Shuchman and LyzengaL 1985). Figure 2 shows 3-D front reconstruction with significant wave heights, and current variations cross front. Figure 2 shows that significant wave variation cross front with maximum significant wave height of 1.2 m and gradient current of 0.9 m/s. March represents the northeast monsoon period as coastal water currents in the South China Sea tend to move from the north direction (Marghany et al., 2010). Nevertheless, Figure 2 shows a meander current with southward direction. In fact, this current is created because of the water inflow from Kuala Terengganu Mouth River. Furthermore, Marghany (1994) and Marghany and Mazlan (2010) quoted that strong tidal current is a dominant feature in the South China Sea with maximum velocity of 1.5

m/s. Clearly, 3-D front coincides with water depth range between 10 to 20 m (Figure 3). Marghany (1994) found that the thermocline and halocline layers occurred in water depth of 20 m. This means that the front occurred between well mixed and stratified water column.

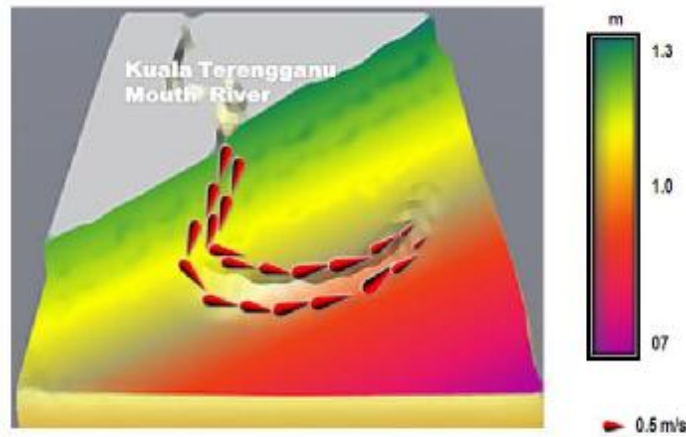


Figure 2: 3-D Front Reconstruction with Significant Wave Height (H_s) and Surface Current Variations (U_y)

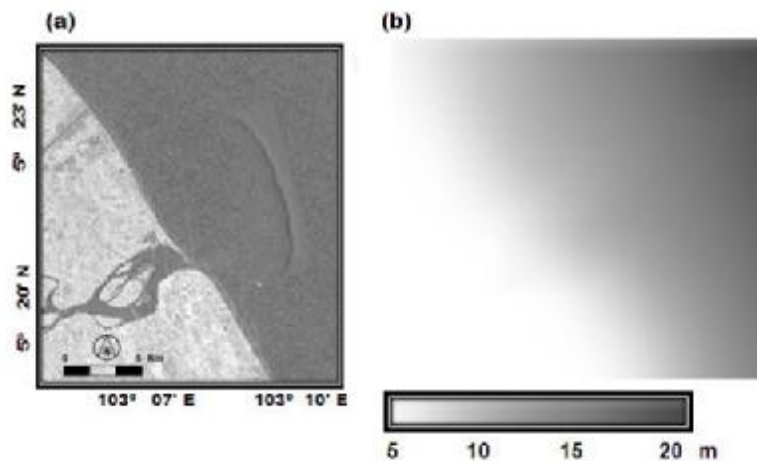


Figure 3: F1 mode data for (a) 3-D front and (b) coastal bathymetry

The visualization of 3-D front is sharp with the RADARSAT-1 SAR C_{HH} band because of each operations on a fuzzy number becomes a sequence of corresponding operations on the respective μ and μ' -levels, and the multiple occurrences of the same fuzzy parameters evaluated as a result of the function on fuzzy variables (Anile 1997). Typically, in computer graphics, two objective quality definitions for Fuzzy B-splines were used: triangle-based criteria and edge-based criteria. Triangle-based criteria follow the rule of maximization or minimization, respectively, the angles of each triangle. The so-called max-min angle criterion prefers short triangles with obtuse angles. In addition, the fuzzy B-spline depicts optimize a locally triangulation between two different points (Anile et al., 1995 and Fuchs et al., 1997). Further, edge-based criteria prefer edges are closely related. This study confirms the previous studies of Anile et al., (1995); Fuchs et al., (1977); Marghany et al., (2010). Indeed, these studies have agreed that fuzzy B-spline algorithm is an accurate tool for 3-D surface reconstruction from 2-D data (Marghany and Mazlan 2011).

CONCLUSION

This work has established procedures to reconstruct 3-D ocean front in RADARSAT-1 SAR F1 mode data. In doing so, three algorithms of velocity bunching, Volterra and fuzzy B-spline are used. The velocity bunching

algorithm modeled significant wave height, Volterra algorithm simulated coastal current movement while fuzzy B-spline implemented the significant wave height to reconstruct 3-D coastal front. The study shows that fuzzy B-spline reconstructed 3-D front with smooth graphic feature with integration of velocity bunching and Volterra algorithm. Indeed, fuzzy B-spline tracked the smooth and rough surface. It can be said that, fuzzy B-spline algorithm can keep track of uncertainty with representing spatially clustered gradient of flow points across the front.

REFERENCES:

- Adeyemo, J. and Fred O. (2009). Optimizing planting areas using differential evolution (DE) and linear programming (LP). *International Journal of Physical Sciences* Vol. 4 (4), pp. 212-220.
- Anile, A. M., (1997). *Report on the activity of the fuzzy soft computing group*, Technical Report of the Dept. of Mathematics, University of Catania, March 1997, pages 10.
- Anile, AM, Deodato, S, Privitera, G. (1995). *Implementing fuzzy arithmetic*, Fuzzy Sets and Systems, 72.
- Anjamrooz, S.H. (2011). Trinity is a numerical model of the holographic universe. *International Journal of the Physical Sciences*, Vol. 6(2), pp. 175-181.
- Anjamrooz, S.H. D.J. McConnell, and H. Azari (2011). The cellular universe: A new cosmological model based on the holographic principle. *International Journal of the Physical Sciences*, Vol. 6(9), pp. 2175-2183.
- Boumaza, N., T. Benouaz, A. Chikhaoui and A. Cheknane (2009). Numerical simulation of nonlinear pulses propagation in a nonlinear optical directional coupler. *International Journal of Physical Sciences* Vol. 4 (9), pp. 505-513.
- Inglada, J. and Garello R., (1999). Depth estimation and 3D topography reconstruction from SAR images showing underwater bottom topography signatures. In *Proceedings of IGARSS'99*.
- Hassasi N. and R. Saneifard (2011). A novel algorithm for solving fuzzy differential inclusions based on reachable set. *International Journal of the Physical Sciences*, Vol. 6(9), pp. 4712-4716.
- Khadijeh M., H. Motameni, R. Enayatifar (2011). New method for edge detection and de noising via fuzzy cellular automata. *International Journal of Physical Sciences* Vol. 6(13), pp. 3175-3180.
- Fuchs H, Kedem ZM, and Useton S.P. (1997). Optimal Surface Reconstruction from Planar Contours. *Commun. of the ACM*. 20: 693-702.
- Majid K. and M. A. Gondal (2011). An efficient two step Laplace decomposition algorithm for singular Volterra integral equations. *International Journal of the Physical Sciences* Vol. 6(20), pp. 4717-4720.
- Marghany M, Mazlan H and Cracknell A.P. (2010). 3-D visualizations of coastal bathymetry by utilization of airborne TOPSAR polarized data. *Int. J. of Dig. Ear.* 3(2):187 – 206.
- Marghany M. and Mazlan H. (2010). Simulation of sea surface current velocity from synthetic aperture radar (SAR) data. *International Journal of the Physical Sciences* Vol. 5(12), pp. 1915-1925.
- Marghany M. and Mazlan H. (2011). Optical digital sensor for three-dimensional turbulent flow visualization. *International Journal of the Physical Sciences* Vol. Vol. 6(3), pp. 506-510.
- Marghany M. (2011). Three-dimensional coastal water front reconstruction from RADARSAT-1 synthetic aperture radar (SAR) satellite data. *International Journal of the Physical Sciences* Vol. 6(29), pp. 6653-6659.
- Marghany M. (2012). Intermonsoon water mass characteristics along coastal waters off Kuala Terengganu, Malaysia. *International Journal of Physical Sciences*. Vol. 7(8), pp. 1294 – 1299.
- Mehmet. K. (2009). An analytical expression for arbitrary derivatives of Gaussian functions $\exp(ax^2)$. *International Journal of Physical Sciences* Vol. 4 (4), pp. 247 – 249.

Messaoudi, M., L. Sbita and M. N. Abdelkrim (2007). A robust nonlinear observer for states and parameters estimation and on-line adaptation of rotor time constant in sensor less induction motor drives. *International Journal of Physical Sciences* Vol. 2 (8), pp. 217-225.

Murat K. K. (2011). Weakened Mannheim curves. *International Journal of the Physical Sciences*, Vol. 6(20), pp. 4700–4705.

Mustafa B. (2011). Natural lift curves and the geodesic sprays for the spherical indicatrices of the involutes of a time like curve in Minkowski 3-space. *International Journal of the Physical Sciences* Vol. 6(20), pp. 4706–4711.

Stephen E. U. (2009). Modified-accelerated Krawczyk's algorithm. *International Journal of Physical Sciences* Vol. 4 (2), pp. 047-052.

Vachon, P.W., Krogstad, H.E., and Paterson, J.S., (1994). Airborne and spaceborne synthetic aperture radar observations of ocean waves. *Atmosphere-Ocean*. 32(10): 83-112.

Ugwu, E. (2009). Analytical study of electromagnetic wave scattering behaviour using Lippmann-Schwinger equation. *International Journal of Physical Sciences* Vol. 4 (5), pp. 310-312.

Zaki, M. S. (2007). On asymptotic behaviour of a second order delay differential equation. *International Journal of Physical Sciences* Vol. 2 (7), pp. 185-187.